Hindawi
International Journal of Photoenergy
Volume 2022, Article ID 5177859, 7 pages
https://doi.org/10.1155/2022/5177859

Research Article

Phytosynthesis of TiO_2 Nanoparticles Using *E. crassipes* Leaf Extracts, Their Photocatalytic Evaluation and Microbicide Effect

A. Monserrat Velázquez-Hernández,[1,2] **José Luis García-Rivas**,[1] **Sonia Martínez-Gallegos**,[1] **Julio César González-Juárez**,[1] **Pablo Schabes-Retchkiman**,[2] **and Verónica Albiter**[1]

[1]*Tecnológico Nacional de México, Instituto Tecnológico de Toluca, División de Estudios de Posgrado e Investigación, Av. Tecnológico S/N Col. Agrícola Bellavista, C.P. 52149, Metepec, Mexico*
[2]*Instituto de Física, Universidad Nacional Autónoma de México, Circuito de la Investigación Científica Ciudad Universitaria, C.P. 04510, CDMX, Mexico*

Correspondence should be addressed to Sonia Martínez-Gallegos; soniazteca@hotmail.com

Received 1 August 2022; Revised 1 November 2022; Accepted 11 November 2022; Published 7 December 2022

Academic Editor: Elias Stathatos

Copyright © 2022 A. Monserrat Velázquez-Hernández et al. This is an open access article distributed under the Creative Commons Attribution License, which permits unrestricted use, distribution, and reproduction in any medium, provided the original work is properly cited.

In the present research work, the photocatalytic and microbicidal activities of titanium nanoparticles (TiO_2 NPs) were evaluated. TiO_2 NPs were obtained through the phytosynthesis process, using *Eichhornia crassipes* leaf extract. In order to determine whether particle size improves photocatalytic and microbicidal activities, the pH of the photosynthesized was modified to 12, 7, and 4. The TiO_2 NPs modified were characterized by UV-Vis spectroscopy (UV-Vis), Fourier transform infrared spectroscopy (FT-IR), and high-resolution transmission electron microscopy (HR-TEM) to reveal the crystalline and morphological nature of the phytosynthesized TiO_2 NPs. UV-Vis analysis revealed that the wavelength for the TiO_2 NPs was 327 nm, while FT-IR confirmed the presence of TiO_2 NPs at peaks located between 536 and 532 cm^{-1}. Finally, HR-TEM analysis showed that all nanoparticles had a TiO_2 composition and a particle size ranging from 25 to 35 nm. For the photocatalytic and microbicidal tests, three concentrations of nanoparticles were used (100, 50, and 10 mg/L), and the results showed that TiO_2 nanoparticles at a concentration of 10 $mg{\cdot}L^{-1}$ demonstrated excellent photocatalytic activity in photodegrading phenol [10 $mg{\cdot}L^{-1}$] up to 98.7%, while their microbicidal activity was more effective in contact with *S. aureus* than with *E. coli*, using a TiO_2 NPs concentration of 100 $mg{\cdot}L^{-1}$.

1. Introduction

Titanium dioxide is a semiconductor material with excellent light transmission, high refractive index, and good dielectric properties [1]. Because it is not harmful to the environment and humans, it has been widely studied, but more importantly, it is used in various fields, such as medicine, cosmetics, optics [2], the packaging industry, as well as pigments in paints, inks, and coatings [3], photocatalysts, and as an antibacterial agent [4].

In general, TiO_2 NPs are an important semiconductor material with a large specific surface area and special chemical properties such as easy control, limited cost, nontoxicity, and resistance [5]. They are the best photocatalytic and microbial agents because of their environmental friendliness, low cost, high oxidative capacity, and chemical and thermal safety against photocorrosion [4].

Freshwater pollutants include bacterial microorganisms, as well as simple and complex chemicals [6]. Phenol and its derivatives are typical pollutants in wastewater and effluents from various industries, including petrochemicals, pharmaceuticals, textiles, pesticides, resins, manufacturing, steel, and herbicides [7, 8].

However, the environmental policy regarding the quality of discharged effluents is increasingly tight, which leads to the need for new resolutions for the water process. Advanced oxidative processes (AOPs) are promising techniques that have the potential to be used as alternative processes or

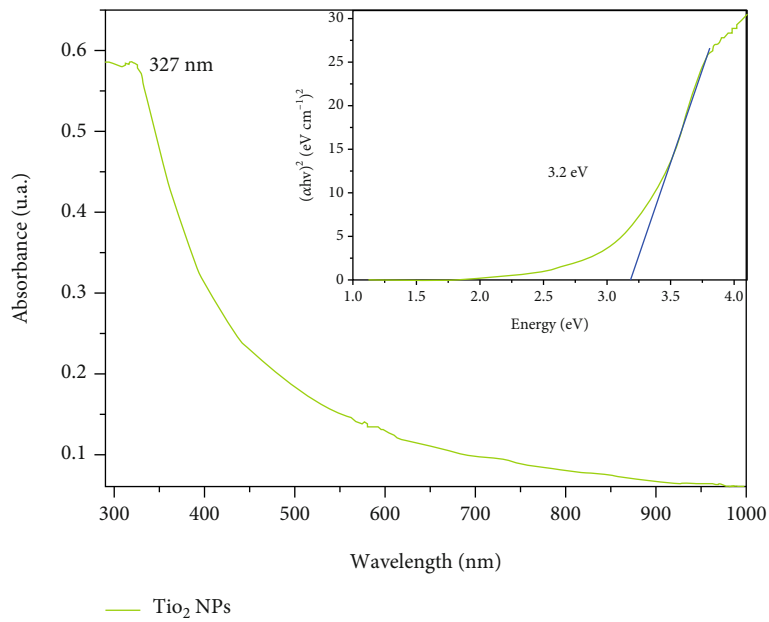

Figure 1: UV-Vis absorption spectrum and Tauc diagram (a) for the bandgap energy measurement.

polishing steps in the effluent process [9]. Heterogeneous photocatalysis using semiconducting metal oxides, such as TiO_2 NPs, is an effective and promising approach to water purification [8, 10].

The main mechanism of heterogeneous photocatalysis is based on the illumination of the photocatalyst (TiO_2 NPs) with the light of appropriate wavelength, with an energy that is equal to or greater than the bandgap, giving rise to the creation of electron/hole (e-/h+) pairs at the conduction (CB) and valence bands (VB), respectively. The photogenerated charges can react with the adsorbed H_2O (OH-) and O_2 molecules on the semiconductor surface where it participates in redox reactions to form OH•- and O_2•- radicals, which are the active species in the photodegradation process, for removing organic contaminants by converting them into CO_2, H_2O, and inorganic ions [4, 8–10].

The antimicrobial activity of nanoparticles is strongly influenced by various intrinsic components such as their morphology, size, chemistry, source, and nanostructure, and the function of interaction with cells, their structures, and cellular metabolites [11]. Specifically, the antimicrobial activity of TiO_2 NPs strongly depends on the photocatalytic performance of TiO_2, which is highly dependent on its morphological, structural, and textural characteristics [1].

Biosynthesis, as a means of synthesizing metal oxide nanoparticles, has proven to be one of the best synthetic processes, primarily because of its environmentally friendly principles and the potential to create new custom materials [7]. Phytosynthesis is considered a safe, cost-effective, biocompatible, nontoxic, sustainable, and environmentally friendly process [1]. The phytochemicals constituents of leaves of *Eichhornia crassipes* like tannins, alkaloids, flavonoids, saponins, and phenolic compounds [12, 13].

In this study, the synthesis of TiNPs using *Eichhornia crassipes* plant extract was conducted. Their photocatalytic and antibacterial activities were investigated by measurement of the degradation of phenol and bacteria (*E. coli* and *S. aureus*), respectively, was investigated.

2. Materials and Methods

2.1. Phytosynthesis of Nanoparticles. *Eichhornia crassipes* were collected from at the Valsequillo reservoir in Puebla. The leaves were washed and dehydrated in a Riossa H-33 drying oven at 50°C for 36 h. About 125 mg of the *E. crassipes* leaf was mixed with ethanol (80% v/v). The aqueous solution was then filtered, and its filtrate was mixed with TiO_2 (0.1 M, Sigma–Aldrich, anatase). Using solutions of NaOH (0.1 M, J.T. Baker) and HNO_3 (0.1 M, J.T. Baker), the pH = 12, 7, and 4 to stablish the pH effect [14, 15] were modified, respectively, and the new solutions were homogenized in an ultrasonic bath (Bransonic Emerson; Model: M2800H). The modified nanoparticles (NPs) at pH 12, 7, and 4 values were separated from the supernatant through centrifugation (Frontier 5714 OHAUS; Model: FC571) at 5000 pm. The supernatant was decanted, and the precipitate was collected, keeping it at room temperature in a desiccator, inside amber bottles, in the dark, for later analysis.

2.2. Characterization. The present study has described the synthesis of TiO_2 NPs by the *E. crassipes* leaf extract. The surface plasmon resonance (SPR) of the phytosynthesized nanoparticles was examined by using UV-Vis spectroscopy (Thermo Scientific Evolution Array) in the range of 300–700 nm. Indirect bandgap energies were determined by the Tauc equation (Equation (1)) that was used to find the energy bandgap as a function of the absorption coefficient and excitation of the transmission [16]

$$(\alpha \bullet h\nu)^{1/\gamma} = \beta\left(h\nu - E_g\right), \quad (1)$$

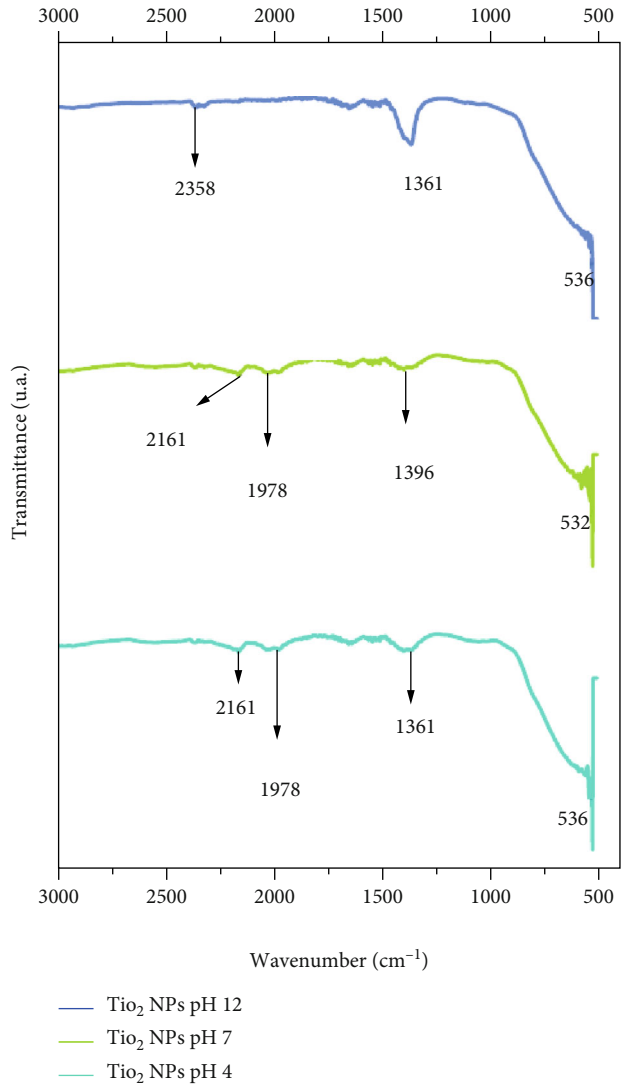

Figure 2: FT-IR spectroscopy analysis for TiO_2 NPs at pH 12, 7, and 4, phytosynthesized with extract of *E. crassipres* leaf.

where α is the extinction coefficient, $h\nu$ is the photon energy, γ is a constant that can take any integer value based on the raw material and the optical transmission values β is the constant and has different values for different transitions, and E_g is the energy gap [16–19].

The bioactive functional groups of TiO_2 NPs were confirmed by Fourier Transform Infrared (FT-IR) analysis (Varian 640–IR with ATR of the diamond), in the range of 4000 to 500 cm^{-1}. Morphology, particle size distribution, and crystallinity were conducted using Transmission Electron Microscopy (TEM–2010 FEG); Micrograph Digital software was used to determine the average particle size of tips.

2.3. Photocatalytic Degradation of Phenol. The photocatalytic activity of the synthesized materials was evaluated by monitoring the degradation of phenol (10 mg·L^{-1}). The photocatalytic degradation of phenol (determined by 4-aminoantipyrine method for total phenols at $\lambda = 510$ nm) at three different concentrations (100, 50, and 10 mg·L^{-1} of TiNPs), at a standard dose of 1 g·L^{-1}. A solution with TiO_2 NPs was initially stirred for 1 h in the absence of light to obtain an adsorption-desorption equilibrium. UV irradiation was provided by one UVA lamp (UVP UVL–18 EL, $\lambda = 254$ nm, 8 w) into a lab-made photoreactor, placed at 10 cm from the samples. During the photocatalytic experiments, at precise time intervals, samples were taken out at regular time intervals, and the nanoparticles were separated from the aqueous solution by a nitrocellulose membrane of 0.45 μm (Whatman), and the supernatant solution was measured to determine the phenol decomposition rate using the UV-Vis spectrophotometer. The solution was purged with air all the time to dissolve oxygen.

The percentage of photodegradation of phenol can be estimated using the following equation:

$$D(\%) = \left(\frac{C_o - C_t}{C_o}\right) \times 100, \quad (2)$$

where C_o is the initial concentration of phenol and C_t is the concentration of phenol after photoirradiation at a given time t [4, 7].

The Langmuir–Hinshelwood kinetics model was used to study the kinetics of the photocatalytic reaction on the surface of TiO_2 NPs, the equation is as follows:

$$\ln\left(\frac{C_o}{C_t}\right) = \mathrm{Kt}, \quad (3)$$

where C_o and C_t represent the concentration of phenol before degradation (C_o) and at different times during photocatalytic degradation (C_t), respectively [4, 5, 7].

2.4. Microbiological Activity of TiO_2 NPs. The antibacterial activity of TiO_2 NPs was tested against the Gram-negative bacteria *Escherichia coli* (ATCC 25922) and Gram-positive *Staphylococcus aureus* (ATCC 6538), using the method established in the Official Mexican Standard [20] Goods and Services, methods for the account of aerobic bacteria in plaque. The variable cells on each of the plates were counted by quantifying the UFCs.

3. Results and Discussion

3.1. Characterization of TiNPs. The TiO_2 nanoparticles exhibited surface plasmon resonance (SPR) at a wavelength of 327 nm (Figure 1), and the optical bandgap energy of the sample was calculated at 3.2 eV (Figure 1(a)). Changes in pH (pH 12, 7, and 4) during the synthesis of plant nanoparticles lead to changes in photocatalytic and bactericidal activity, but SPR and bandgap energy remained unchanged [5]. Ziental et al., [21] and Nobijari et al., [8], synthesized TiO_2 nanoparticles with *Monsonia burkeana* extract, and mentioned that the band gap value of 2.3 eV is like that of the anatase TiO_2. This can lead to the production of high-energy electrons. Whole pairs (e-/h) in UVA light with a wavelength of 385 nm or less [1, 9].

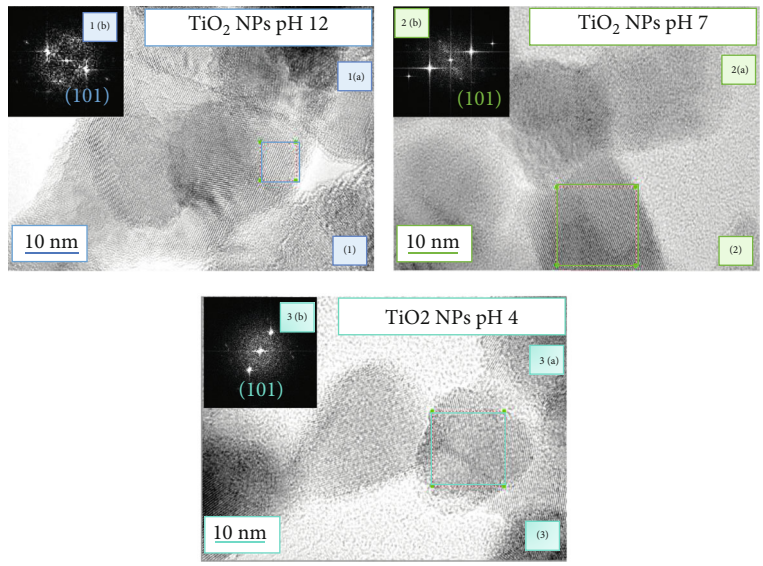

Figure 3: TEM micrographs of TiO_2 NPs and FFT analysis pH 12 (1a, 1b), pH 7 (2a, 2b), and pH 4 (3a, 3b).

FT-IR spectrum of TiO_2 NPs at pH 12, 7, and 4 shown in Figure 2, the peak region of 2161 cm^{-1} showed the presence of stretching bands of the carbonyl group [22], 1396 cm^{-1} corresponds to C-N stretching of the aromatic amide group [23], in general, the absorption bands that appear from 2358 to 1361 cm^{-1} correspond to the phytochemicals present in the extract of *E. crassipes* from Puebla.

For all samples, the peaks identified from 536 to 532 cm^{-1} confirm the formation of TiO_2 nanoparticles, through the phytosynthesis process, the intense band below 1000 cm^{-1} belongs to TiO_2 nanoparticles bridging stretching mode [5, 8]; according to the spectra, the phytochemicals from *E. crassipes* extract act as coating agents in the synthesis of nanoparticles TiO_2 NPs.

The morphology and arrangement of TiO_2 NPs synthesized at pH 12 (Figure 3.1), 7 (Figure 3.2), and 4 (Figure 3.3) shows that the nanoparticles are agglomerated and of undefined shapes, with sizes ranging from 33.5 nm ± 7.5 nm, 30.5 nm ± 6.5 nm, and 25 nm ± 8.5 nm for TiO_2 NPs pH 12, TiO_2 NPs pH 7, and TiO_2 NPs pH 4, respectively. All the phytosynthesized TiO_2 NPs have a tetragonal form, composition of TiO_2, for anatase according to PDF Card 78 2486.

According to the presented characterization results, it is not observed that the used pH value for the synthesis shows a determining influence on the size, shape, or composition of the nanoparticles, these three parameters differ for the three pH values. Similar observations were also reported by Shanavas et al., [24], Thakur et al., [25], Srinivasan et al., [23] whose synthesized nanoparticles with *Phyllanthus niruri*, *Azadirachta indica*, and *Sesbania grandiflora* obtained results similar to those of the present work.

3.2. Photocatalytic Degradation of Phenol. Figure 4 shows the phenol degradation profiles in the presence of TiO_2 NPs pH 12 (Figure 4.1), Ti O_2 NPs pH 7 (Figure 4.2), and Ti O_2 NPs pH 4 (Figure 4.3), at concentrations of 100 $mg{\cdot}L^{-1}$, 50 $mg{\cdot}L^{-1}$, and 10 $mg{\cdot}L^{-1}$ of NPs. Before turning on the light, phenol concentration was observed to drop 0.7 $mg{\cdot}L^{-1}$ at pH 12 and 7, and rise to 2 $mg{\cdot}L^{-1}$ at pH 4 due to its adsorption/desorption on the surface of TiO_2 NPs [8], observing the same phenomenon. After switching on the UV light, the phenol concentration decreases gradually with irradiation time.

According to the relationship of the characterization results for TiO_2 NPs and photocatalytic capacity, no determining influence on photodegradation due to the nanoparticles' size, shape, or composition. Although it cannot be generalized in any of the cases, the main influence is due to the used pH for the phytosynthesis of the nanoparticles, followed by the size diversity, then the composition, and finally the crystalline structure. Regarding the initial phenol concentration, in most photocatalytic tests, the best percentage of degradation is achieved at a lower concentration of nanoparticles.

At concentrations of 100 $mg{\cdot}L^{-1}$, the degradation efficiency of phenol decreases, according to Nobijari et al., [8], when the catalyst concentration is too high, other effects such as light scattering and poor illumination of the photocatalyst particles become dominant.

Langmuir-Hinshelwood's kinetics model was used to study the kinetics of the photocatalytic degradation of phenol. Parameters of adsorption were observed in Table 1. The R^2 values of 0.9284, 0.9443, and 0.9467 that had the best fits were for TiO_2 NPs pH 12–50 $mg\,L^{-1}$, TiO_2 NPs pH 7–100 $mg{\cdot}L^{-1}$, and TiO_2 NPs pH 4–50 $mg{\cdot}L^{-1}$, respectively. The R^2 coefficient value did not indicate a good correlation between the Langmuir and Hinshelwood kinetics model. This observation could be due to the multiple processes taking place during photocatalytic degradation [5].

3.3. Microbiological Activity of TiO_2 NPs. Different concentrations of TiO_2 nanoparticles were tested to determine the inhibitory effect against the model bacterium *Escherichia coli* and *Staphylococcus aureus*. In each test, three different

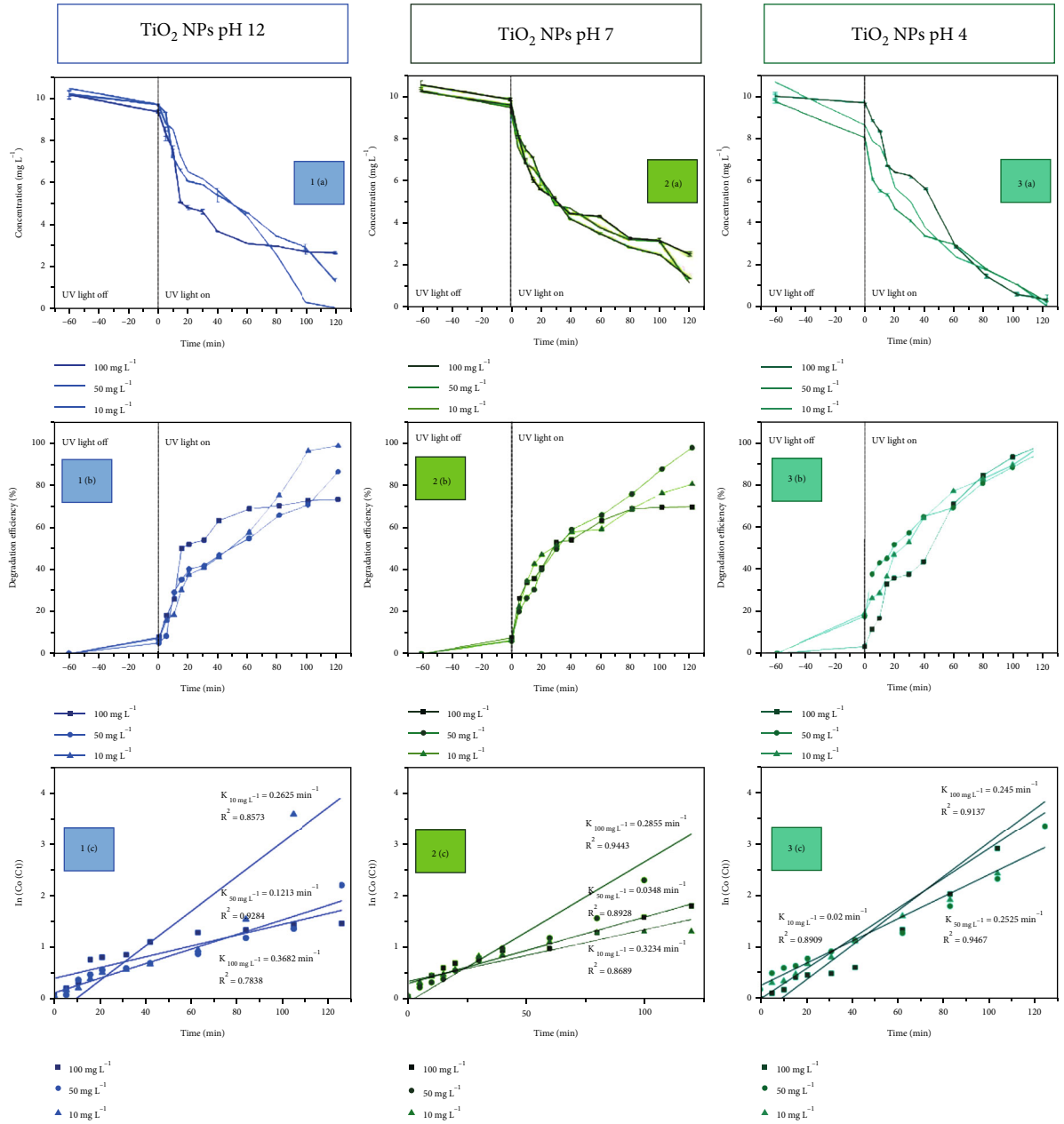

FIGURE 4: Phenol concentration for TiO_2 NPs at pH 12 (1a), 7 (2a), and 4 (3a), degradation efficiency for TiO_2 NPs at pH 12 (1b), 7 (2b), and 4 (3b), and the Langmuir-Hinshelwood kinetics model for TiO_2 NPs at pH 12 (1c), 7 (2c), and 4 (3c).

TABLE 1: Parameters of adsorption for the isotherm models.

	Concentration 100 mg L^{-1}			Concentration 50 mg L^{-1}			Concentration 10 mg L^{-1}		
pH synthesis	K (m^{-1})	R^2	DE (%)	K (m^{-1})	R^2	DE (%)	K (m^{-1})	R^2	DE (%)
12	0.3682	0.7838	73.10	0.1213	0.9284	86.09	0.2625	0.8573	98.57
7	0.2855	0.9443	69.28	0.0348	0.8928	80.01	0.3234	0.8689	97.19
4	0.2450	0.9137	95.16	0.2525	0.9467	98.38	0.0200	0.8909	98.55

concentrations of 100, 50, and 10 mg·L^{-1} of TiO_2 NPs were tested, after seeding the CFU·mL^{-1} and after an incubation period of 24 h, and the results were obtained.

TiO_2 nanoparticles synthesized using *Eichhornia crassipes* leaf extract were found effective against *Escherichia coli* and *Staphylococcus aureus* (Figure 5). Remarkably, TiO_2

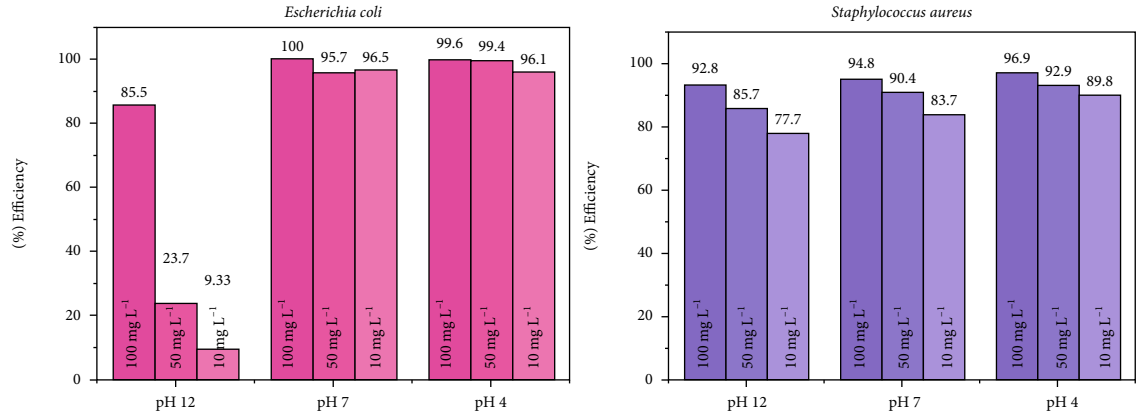

FIGURE 5: Microbiological efficiency of TiO_2 NPs in contact with *Escherichia coli* (Gram-negative) and *Staphylococcus aureus* (Gram-positive).

NPs pH 12 has shown that *E. coli* is the most resistant to TiO_2 NPs in comparison to *S. aureus*. [11] in his study synthesized titanium nanoparticles with extract of *Thalictrum minus L. ssp. Elatum* obtained similar results.

The inhibition of *E. coli* and *S. aureus* by TiO_2 NPs at pH 12, pH 7, and pH 4 presented the best results at concentrations of 100 mg·L^{-1} of nanoparticles, [26], mention that the population of bacteria declined when the concentration of nanoparticles increased. The results showed that Gram-negative are slightly less resistant to TiO_2 nanoparticles compared to Gram-positive, which may be mainly due to differences in the structures of bacterial membranes [1, 27].

TiO_2 NPs interact with the surface of bacterial membranes and alter their cell permeability, penetrate bacterial cells, leading to the generation of ROS (Reactive Oxygen Species), causing damage to the cell membrane, inducing lysis, and consequently giving rise to cell death. Moreover, the antimicrobial activity of TiO_2 NPs is related to their structure, shape, and size, as well as the production of ROS [28].

4. Conclusions

The phytosynthesis of TiO_2 NPs using *Eichhornia crassipes* leaf extracts was ecological, sustainable, cheap, and free of contaminants that satisfy the requirements to be an environmentally friendly process. UV-Vis spectrophotometric analysis reveals that phytosynthesized nanoparticles have values in the appropriate range of 327 nm and 3.2 eV of bandgap energy from the Tauc plot; TiO_2 NPs show significant peaks identified at 538 and 532 cm^{-1} confirming the presence of TiO_2. All the TiO_2 NPs phytosynthesized have a tetragonal form, composition of TiO_2, and particle sizes ranging from 20 to 50 nm; TiO_2 NPs show better photocatalytic efficiencies at acidic pH and concentrations of 10 mg·L^{-1}. Antibacterial activity against Gram-positive and Gram-negative bacteria is efficient at concentrations of 100 mg·L^{-1} for all the TiO_2 NPs phytosynthesized.

Data Availability

All data generated or analyzed during this study are included in this published.

Conflicts of Interest

The authors declare that they have no conflicts of interest.

Acknowledgments

The authors are grateful for the financial support from the National Technological Institute of Mexico (TecNM), the LIIA Instituto Tecnológico de Toluca (ITTol), and the CONACYT doctoral scholarship awarded to Monserrat Velázquez Hernández CVU 788388.

References

[1] C. L. de Dicastillo, M. G. Correa, F. B. Martínez, C. Streitt, and M. J. Galotto, "Antimicrobial Effect of Titanium Dioxide Nanoparticles," in *Antimicrobial Resistance - A One Health Perspective*, IntechOpen, 2021.

[2] S. Nadzirah, U. Hashim, S. C. B. Gopinath et al., "Titanium dioxide–mediated resistive nanobiosensor for *E. coli* O157:H7," *Microchimica Acta*, vol. 187, no. 4, p. 235, 2020.

[3] S. Liu, M. Wang, T. Li, and Q. Chen, "Response of an aerobic denitrifier to titanium dioxide nanoparticles exposure," *Environmental Technology (United Kingdom)*, vol. 41, no. 11, pp. 1446–1454, 2020.

[4] O. Ibukun and H. K. Jeong, "Tailoring titanium dioxide by silver particles for photocatalysis," *Current Applied Physics*, vol. 20, no. 1, pp. 23–28, 2020.

[5] N. M. Ngoepe, M. M. Mathipa, and N. C. Hintsho-Mbita, "Biosynthesis of titanium dioxide nanoparticles for the photodegradation of dyes and removal of bacteria," *Optik*, vol. 224, article 165728, 2020.

[6] O. G. Gómez-Duarte, "Contaminación del agua en países de bajos y medianos recursos, un problema de salud pública," in *Revista Facultad de Medicina*, vol. 66, no. 1pp. 7-8, Universidad Nacional de Colombia, 2018.

[7] S. I. Mustapha, F. A. Aderibigbe, T. L. Adewoye, I. A. Mohammed, and T. O. Odey, "Silver and titanium oxides for the removal of phenols from pharmaceutical wastewater," *Materials Today: Proceedings*, vol. 38, pp. 816–822, 2021.

[8] L. A. Nobijari, M. Schwarze, and M. Tasbihi, "Photocatalytic degradation of phenol using photodeposited Pt nanoparticles on titania," *Journal of Nanoscience and Nanotechnology*, vol. 20, no. 2, pp. 1056–1065, 2020.

[9] I. Levchuk and M. Sillanpää, "Titanium dioxide-based nanomaterials for photocatalytic water treatment," in *Advanced Water Treatment: Advanced Oxidation Processes*, pp. 1–56, Elsevier, 2020.

[10] M. K. Arfanis, C. P. Athanasekou, E. Sakellis et al., "Photocatalytic properties of copper–modified core-shell titania nanocomposites," *Journal of Photochemistry and Photobiology A: Chemistry*, vol. 370, no. June 2018, pp. 145–155, 2019.

[11] E. L. Pavlova, R. D. Toshkovska, T. E. Doncheva, and I. A. Ivanova, "Prooxidant and antimicrobic effects of iron and titanium oxide nanoparticles and thalicarpine," *Archives of Microbiology*, vol. 202, no. 7, pp. 1873–1880, 2020.

[12] G. Anusiya, S. Bharathi, K. Mukesh Praveen, and G. Sainandhini, "Extraction and molecular characterization of biological compounds from water hyacinth," *Journal of Medicinal Plants Studies*, vol. 8, no. 5, pp. 14–19, 2020.

[13] C. N. Rodríguez Pava, A. G. Zarate Sanabria, and L. C. Sánchez Leal, "Actividad antimicrobiana de cuatro variedades de plantas frente a patógenos de importancia clínica en Colombia," *Nova*, vol. 15, no. 27, p. 119, 2017.

[14] J. Abisharani and R. Kumar, "Green synthesis of TiO_2 nanoparticles using Cucurbita pepo seeds extract," *Materials today: proceedings*, vol. 14, pp. 302–307, 2019.

[15] A. Silva, S. Martínez-Gallegos, G. Rosano-Ortega, P. Schabes-Retchkiman, C. Vega-Lebrún, and V. Albiter, "Nanotoxicity for E. coli and characterization of silver quantum dots produced by biosynthesis with Eichhornia crassipes," *Journal of Nanostructures*, vol. 7, no. 1, pp. 1–12, 2017.

[16] R. S. Mahmood, W. Abdulsatar, and M. A. Fakhri, "Synthesis of nano titanium oxide for photonic application," *AIP Conference Proceedings*, vol. 2213, 2020.

[17] S. P. Goutam, G. Saxena, V. Singh, A. K. Yadav, R. N. Bharagava, and K. B. Thapa, "Green synthesis of TiO_2 nanoparticles using leaf extract of *Jatropha curcas* L. for photocatalytic degradation of tannery wastewater," *Chemical Engineering Journal*, vol. 336, pp. 386–396, 2018.

[18] N. Kamarulzaman, M. F. Kasim, and R. Rusdi, "Band gap narrowing and widening of ZnO nanostructures and doped materials," *Nanoscale Research Letters*, vol. 10, no. 1, p. 1034, 2015.

[19] P. Makuła, M. Pacia, and W. Macyk, "How to correctly determine the band gap energy of modified semiconductor photocatalysts based on UV-vis spectra," *Journal of Physical Chemistry Letters*, vol. 9, no. 23, pp. 6814–6817, 2018.

[20] NOM-092-SSA1-1994, "NOM-092-SSA1-1994, Bienes y servicios," in *Método para la cuenta de bacterias aerobias en placa*, vol. 12, pp. 1–6, Diario Oficial de La Federación, 1995.

[21] D. Ziental, B. Czarczynska-Goslinska, D. T. Mlynarczyk et al., "Titanium dioxide nanoparticles: prospects and applications in medicine," in *nanomaterials*, vol. 10, no. 2, 2020MDPI AG, 2020.

[22] L. Wang, J. Xu, Y. Yan, H. Liu, T. Karunakaran, and F. Li, "Green synthesis of gold nanoparticles from *Scutellaria barbata* and its anticancer activity in pancreatic cancer cell (PANC-1)," *Artificial cells, nanomedicine, and biotechnology*, vol. 47, no. 1, pp. 1617–1627, 2019.

[23] M. Srinivasan, M. Venkatesan, V. Arumugam et al., "Green synthesis and characterization of titanium dioxide nanoparticles (TiO_2 NPs) using *Sesbania grandiflora* and evaluation of toxicity in zebrafish embryos," *Process Biochemistry*, vol. 80, pp. 197–202, 2019.

[24] S. Shanavas, A. Priyadharsan, S. Karthikeyan et al., "Green synthesis of titanium dioxide nanoparticles using *Phyllanthus niruri* leaf extract and study on its structural, optical and morphological properties," *Materials Today: Proceedings*, vol. 26, pp. 3531–3534, 2020.

[25] B. K. Thakur, A. Kumar, and D. Kumar, "Green synthesis of titanium dioxide nanoparticles using *Azadirachta indica* leaf extract and evaluation of their antibacterial activity," *South African Journal of Botany*, vol. 124, pp. 223–227, 2019.

[26] M. Alizadeh-Sani, H. Hamishehkar, A. Khezerlou et al., "Kinetics analysis and susceptibility coefficient of the pathogenic bacteria by titanium dioxide and zinc oxide nanoparticles," *Advanced Pharmaceutical Bulletin*, vol. 10, no. 1, pp. 56–64, 2020.

[27] S. Subhapriya and P. Gomathipriya, "Green synthesis of titanium dioxide (TiO_2) nanoparticles by *Trigonella foenum-graecum* extract and its antimicrobial properties," *Microbial Pathogenesis*, vol. 116, pp. 215–220, 2018.

[28] S. Albukhaty, L. Al-Bayati, H. Al-Karagoly, and S. Al-Musawi, "Preparation and characterization of titanium dioxide nanoparticles and *in vitro* investigation of their cytotoxicity and antibacterial activity against *Staphylococcus aureus* and *Escherichia coli*," *Animal Biotechnology*, vol. 33, no. 2, 2022.